

# **SPITZER SPACE TELESCOPE: OBSERVATORY DESCRIPTION AND PERFORMANCE**

**Keyur C. Patel**

Spitzer Flight Engineering Office Manager, Jet Propulsion Laboratory

**Stuart R. Spath**

Spitzer Observatory Engineering Manager, Lockheed Martin Space Systems Company

The Spitzer Space Telescope, the last of the four Great Observatories commissioned by the National Aeronautics and Space Administration, was successfully launched on August 25, 2003 from Kennedy Space Center. The engineering systems for Spitzer were developed by the Jet Propulsion Laboratory, Lockheed Martin Space Systems Company, and Ball Aerospace & Technology Corp. This paper provides an overview of Spitzer, a technical description of all the engineering subsystems, and the associated challenges involved in developing them to satisfy the mission requirements. In addition, this paper describes the performance of the engineering subsystems during the In-Orbit Checkout phase, the Science Verification phase, and the early portions of the Nominal Mission.

## **INTRODUCTION**

The Spitzer Space Telescope, formerly known as the Space Infrared Telescope Facility (SIRTF), was commissioned by the National Aeronautics and Space Administration (NASA) to collect infrared science data of unprecedented quality and quantity. It was developed as the final component of the Great Observatories program, joining the Hubble Space Telescope, the Chandra X-ray Observatory, and the Compton Gamma Ray Observatory. In addition, Spitzer is a scientific and technical cornerstone of NASA's Origins program. The project made use of some of the nation's premier technologies in fundamental scientific applications such as the search for other solar systems and studies of the earliest stages in the formation of galaxies similar to our own Milky Way. The immense potential of this mission was built upon the large defense-based investment in infrared detector arrays, with additional development under NASA sponsorship. Although the astronomical community has benefited from the breakthroughs in these arrays, their performance is degraded by factors of 100 to 1000 due to the heat radiation encountered on ground-based telescopes. Only with a cryogenically cooled telescope in space can the full potential for discovery be realized. Infrared observations are important for the following reasons: they reveal cool states of matter, they explore the universe hidden by cosmic dust, they access a wealth of spectral features, and they reach back to the early existence of the cosmos.

Although the science capabilities of Spitzer are unparalleled, this paper does not discuss the details of the science instruments nor the science data collected thus far in the mission. Instead, it focuses on the engineering subsystems on-board the Observatory, both in the spacecraft (S/C) and the Cryogenic Telescope Assembly (CTA). The Observatory performance has been nothing short of exceptional. Using a subsystem-by-subsystem approach, this paper describes the design characteristics of the various components. It discusses significant subsystem challenges encountered during the development phase. It also contains a block diagram or schematic for each subsystem, illustrating the important hardware and software components. Finally, this paper documents the in-flight performance of each subsystem.

## MISSION OVERVIEW

**Mission Trajectory.** Spitzer was launched into an Earth-trailing solar orbit rather than a more conventional Earth orbit used by the other Great Observatories. The solar orbit was selected for a number of reasons: a) low launch energies allow for significant mass savings, b) the Observatory leaves behind the Earth's trapped radiation environment, c) Earth/Moon avoidance constraints are simplified, d) propellant for station-keeping or trajectory correction is not required, e) deep space tracking is simplified, and f) heat input from the Earth is eliminated, providing a vast improvement in the quality of the infrared observations.

**Mission Phases.** Following launch, the Observatory was initialized and commissioned for routine operations during a 62-day period called In-Orbit Checkout (IOC) phase. The emphasis for the IOC phase was to bring the Observatory on-line safely, verify functionality of the instruments, telescope, and spacecraft, and demonstrate that the facility meets all level-1 requirements. After IOC, there was a 30-day period called the Science Verification (SV) phase. The purpose of the SV phase was to characterize the Observatory in-orbit performance, demonstrate capability for autonomous operations, conduct early release observations, and exercise the ground systems software, processes, and staffing sufficiently to commission the facility for routine operations. Following the SV phase, the Observatory began the Nominal Mission phase, which is expected to continue for at least the next 5 years.

**Uplink/Downlink Strategy.** During the Nominal Mission phase, commanding is performed primarily by uplinking a new master sequence once per week. The master sequence commands the science observations, the engineering calibrations, and the data playbacks. The sequence prioritizes the playbacks of the various science and engineering data. Spitzer playbacks occur twice per day, and are one hour or less in duration. While the duration can vary, the average playback provides up to 700 Mbytes of engineering and science data. When data is lost during transmission, a ground process is used to create a command file to retransmit the missing data.

## OBSERVATORY DESCRIPTION AND SYSTEM OVERVIEW

The Observatory consists of five primary systems: the Spacecraft (S/C), the Cryogenic-Telescope Assembly (CTA), and three science instruments: the Infrared Array Camera (IRAC), the Infrared Spectrograph (IRS), and the Multiband Imaging Photometer for Spitzer (MIPS). The S/C is comprised of the solar panel, the S/C bus, and various support structures. The S/C bus contains the hardware and software for the following engineering subsystems: Command & Data Handling (C&DH), Pointing Control Subsystem (PCS), Reaction Control Subsystem (RCS), Power Generation & Distribution (PG&D), Telecommunications Subsystem (Telecom), and Thermal Control Subsystem (TCS). The Flight Software (FSW) resides in the flight processor card of the C&DH and provides all the algorithms, parameters, and fault protection required by these subsystems.

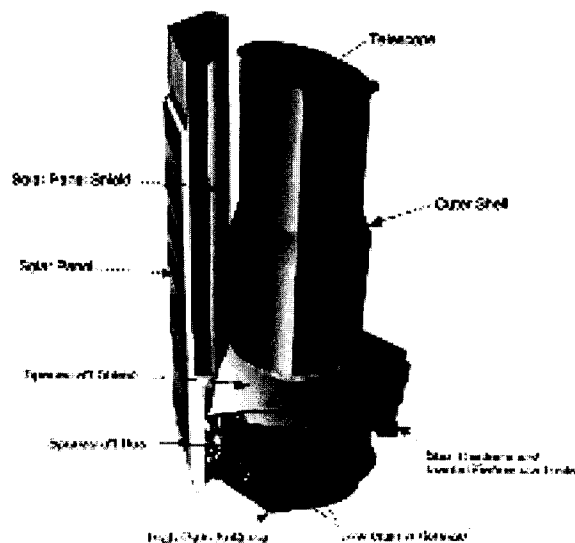


Figure 1. Observatory External Configuration



**In-Flight Performance.** The performance of the C&DH subsystem has been nominal. The MMCs have been storing the required science and engineering data onboard without problems, and a ground-based process is being used effectively to keep adequate free space on the MMCs. Average FPC utilization has been 52%, with peaks up to 94%. All other C&DH components are functioning well with no concerns of any kind.

## POINTING CONTROL SUBSYSTEM (PCS)

**Subsystem Overview.** PCS provides two main functions: pointing the Observatory to the desired orientation (pointing control) and estimating the current attitude of the Observatory (attitude determination). Pointing control is achieved via a celestial-inertial, three-axis stabilized control system using four Reaction Wheels Assemblies (RWA), which are periodically desaturated with cold-gas nitrogen thrusters. Attitude determination is obtained using the following sensors: Star Tracker Assemblies (STA), Inertial Reference Units (IRU), Pointing Calibration Reference Sensors (PCRS), and Wide Angle Sun Sensors (WASS). All the PCS components are redundant and are cross-strapped to the C&DH to provide maximum fault tolerance. Due to the very tight pointing requirements for Spitzer, significant PCS software algorithms are used to provide the best overall performance. Descriptions of the various PCS elements are shown below.

**Reaction Wheel Assembly (RWA).** Four RWAs provide the control actuation for all modes of operation. They are mounted in a pyramid orientation about the telescope boresight axis, each canted at 30°. RWA sizing was driven by the need to provide sufficient capacity for quick repositioning as well as large angle slews. Each reaction wheel provides torque up to 0.04 N-m and momentum storage capacity of 19 N-m-sec.

**Star Tracker Assembly (STA).** The STA obtains attitude knowledge through autonomous identification of stars carried in an extensive on-board catalog of about 87,000 stars. The STA provides star position measurements at 2 Hz to an absolute accuracy (1 $\sigma$ ) of 1.5 arcsec per axis per star, with a noise equivalent angle (1 $\sigma$ ) of 0.75 arcsec per axis per star. The field of view is 5° x 5°, driven by the need to ensure a minimum of 4 stars at the galactic poles.

**Inertial Reference Unit (IRU).** The IRU employs two dual-axis spinning-mass gyros to measure the angular rate of the Observatory relative to inertial space. The IRU provides performance capable of achieving 0.4 arcsec relative accuracy in the incremental pointing mode. For absolute attitude estimates, the IRU output must be periodically tied back to inertial space using the STA. To obtain the best performance from the IRU, the PCS employs an 18-state Kalman filter known as the Gyro Calibration Filter (GCF), which continually estimates scale factor, alignment, and bias. A detailed IRU calibration sequence is performed in flight once every three days to allow the GCF to produce its estimates. The GCF output is sampled and latched for use in correcting subsequent gyro readings.

**Pointing Calibration and Reference Sensor (PCRS).** All telescope pointing is defined and calibrated relative to the PCRS located on the telescope focal plane in the CTA. During the mission, the PCRS is periodically used to calibrate the telescope-to-spacecraft alignment that may drift due to thermo-mechanical or other slowly varying effects. The PCRS cold assembly operates at 1.4K and dissipates less than 0.1 mW of heat into the cryostat. The detector is a 4 x 4 Silicon PIN photodiode array. Each pixel is 250  $\mu$ m square, with a plate scale of 10 arcsec per pixel. PCRS calibration is performed by centering a target star onto the middle four pixels of the array, resulting in an accuracy (1 $\sigma$ ) of 0.1 arcsec per axis.

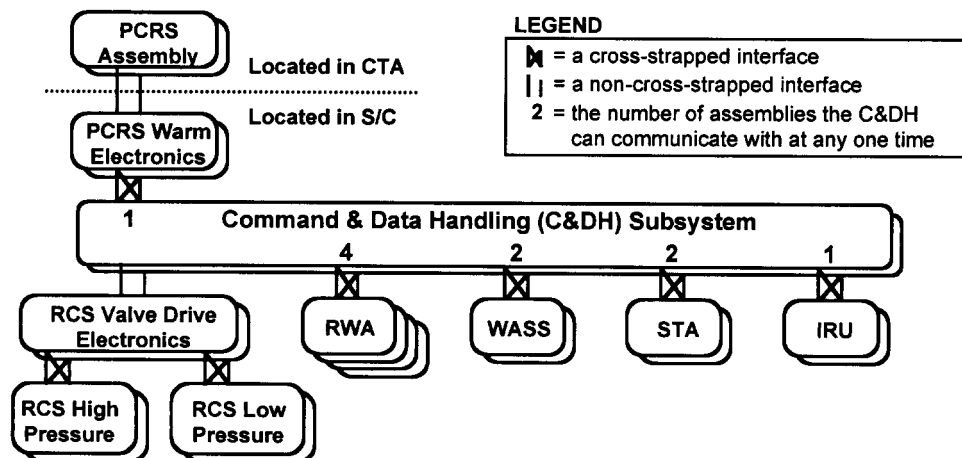


*Figure 3. Pointing Control Subsystem Block Diagram*

**Wide Angle Sun Sensor (WASS).** Two externally mounted WASS's measure sun position with respect to the Observatory. Each WASS provides a field of view of  $2\pi$  steradians with an accuracy of  $\pm 0.26^\circ$  at null. They are placed at the top and the bottom of the sun shield to minimize viewing obstructions, with their boresights aligned to the spacecraft solar array normal. The WASS's are used by fault protection during nominal modes to ensure that the cryogenically cooled telescope remains shaded by the solar array at all times. In addition, the WASS's are used during Safe Mode as the primary control sensors, thus eliminating dependence on the STA.

**In-Flight Performance.** In all areas, the PCS in-flight performance meets or exceeds the subsystem requirements. Flight telemetry has shown the ability of the PCS to scan at a constant 2 arcsec/sec rate with an root-mean-square stability of 0.042 arcsec over 15 seconds, and 0.048 arcsec over 150 seconds. Tracking performance for solar-system objects has been demonstrated at rates between 0.002 and 1.0 arcsec/sec, with less than 1.0 arcsec error. Pointing accuracy has been confirmed by examining the centroids produced during the PCRS calibrations. The root-mean-square radial error is less than 0.5 arcsecond, a portion of which is noise in the PCRS. Because these readings are taken just before recalibration, the measurements indicate an upper bound on the actual pointing error using the star tracker.

Because it is important to point specific science instruments at celestial objects, the precise offsets between the telescope boresight and each instrument's boresight must be known. During IOC, a focal plane survey mapped the positions of each sensor, and in some cases, multiple points on a given sensor, with respect to the PCRS. The offsets were determined through ground processing with a Kalman filter, and the results are stored onboard in a frame table. Each of the 128 entries in this table is a quaternion relating a particular instrument-pointing frame to the telescope-pointing frame.

## **REACTION CONTROL SUBSYSTEM (RCS)**

**Subsystem Overview.** The RCS provides the impulse required to unload the accumulated angular momentum in the reaction wheels, and operates under control commands initiated from the Pointing Control Subsystem. The RCS is a nitrogen cold gas system. With the exception of pressure vessels and tubing, the entire subsystem is fully redundant. The RCS hardware includes the following:

**Propellant Tank.** A single 48.3 cm diameter propellant tank stores 15.6 kg of gaseous nitrogen, sufficiently large to compensate for the effects of one-sided torques such as solar pressure and helium venting. The nitrogen supply provides an on-orbit design lifetime of 5.2 years with substantial margin. Nominal tank pressure at beginning of life is 4250 psi. A propellant feed/isolation system reduces the absolute propellant pressure to 100 psi at the thrusters.

**Cold Gas Thrusters.** A redundant two-branch configuration with twelve 0.12 N cold gas thrusters (6 thrusters per branch) provides the forces and moments in all three axes required to unload the RWA momentum.

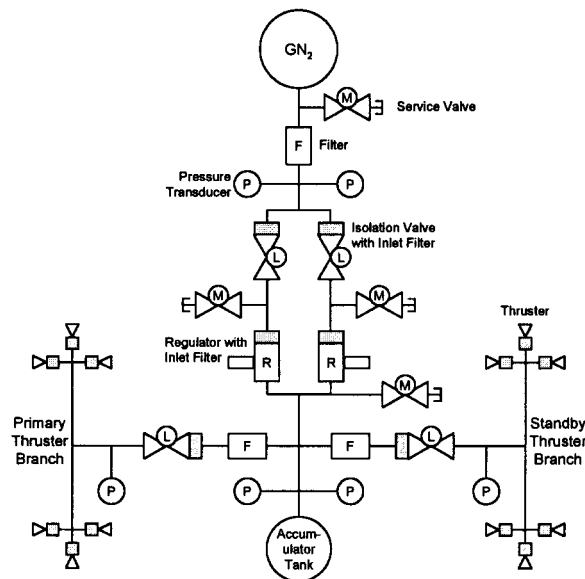


Figure 4. Reaction Control Subsystem Schematic

**Isolation Valves.** Two high-pressure and two low-pressure isolation valves separate the regulators and thruster branches. These valves have an increased importance due to thruster leak concerns.

**Miscellaneous Hardware.** Also included in the RCS design are two regulators, an accumulator tank, tubing, and multiple pressure transducers, system filters, and service valves.

**Development Challenges.** A key development challenge was presented by the thrusters, which exhibited a characteristic of varying levels of intermittent leakage. An investigation for root cause led to the conclusion that the leakage was caused by self-generated particulates from a thruster's sliding-fit poppet. Extensive cycle testing of spare units gave confidence that the thrusters would not seize during flight, and the decision was made to fly with the thrusters. The project concluded that the mission could be conducted even with significant thruster leakage because the placements of the isolation valves minimize the loss of propellant. In addition, methods of spacecraft operation that reduced the number of thruster cycles were developed and implemented, and contingency plans were developed to further reduce risk.

**In-Flight Performance.** All RCS telemetry and post-desaturation analysis results have been as expected. The thruster leaks observed in ground tests have also been seen during flight with post-desaturation leak rates ranging from 20 to 670 scc/hr. These leak rates are acceptable because they are well below the concern level of 5000 scc/hr, and because the lost 0.6 g of nitrogen per desaturation event is negligible. Consumable analysis for the nitrogen shows that there is about 200% margin on the 5.2-year mission goal.

## POWER GENERATION AND DISTRIBUTION (PG&D) SUBSYSTEM

**Subsystem Overview.** The PG&D subsystem provides electrical power generation, energy storage, and power distribution for the Observatory. The PG&D design is a direct energy transfer system where the solar array and battery are connected directly to a  $28\text{ V} \pm 6\text{ V}$  power bus. The PG&D ensures that there is an energy balance between the loads drawn by the powered equipment and the supply available from the solar array and/or the battery. All components in the PG&D are either fault tolerant (e.g., solar array assembly, charge control unit, battery assembly) or block redundant (e.g., power distribution and drive unit). Fault tolerance with respect to shorts to structure is accomplished through the use of a balanced bus single point grounding method that is single fault tolerant with respect to shorts to structure anywhere on the Observatory.

**Solar Panel Assembly.** The solar panels provide 500 W of power at the beginning of life and 449 W at the end of life (5.2-years after launch), assuming the failure of one string. The solar panel assembly consists of two solar panels with a total solar cell area of  $2.8\text{ m}^2$ . The entire assembly is configured with 14 strings of circuits consisting of 784 cells. Fault isolation in the form of blocking diodes is used to protect the individual strings.

**Battery Assembly.** The battery assembly provides electrical power from launch through the ascent phase and during periods when the power needs are more than the solar panels can provide. The battery charge capacity is 16 Amp-hours, and it is sized to provide 240 W average for 60 minutes with less than 60% depth-of-discharge.

**Power Distribution and Drive Unit (PDDU).** The PDDU works in conjunction with the solar array and the charge control unit to maintain the battery charge and to provide power to the selected loads through solid-state current limited switches. The PDDU also provides discrete input/output and analog inputs as an extension to the C&DH.

**Charge Control Unit (CCU).** The redundant CCU provides charge control for the battery, load current to the spacecraft bus via the PDDU, and power acquisition telemetry to the spacecraft.

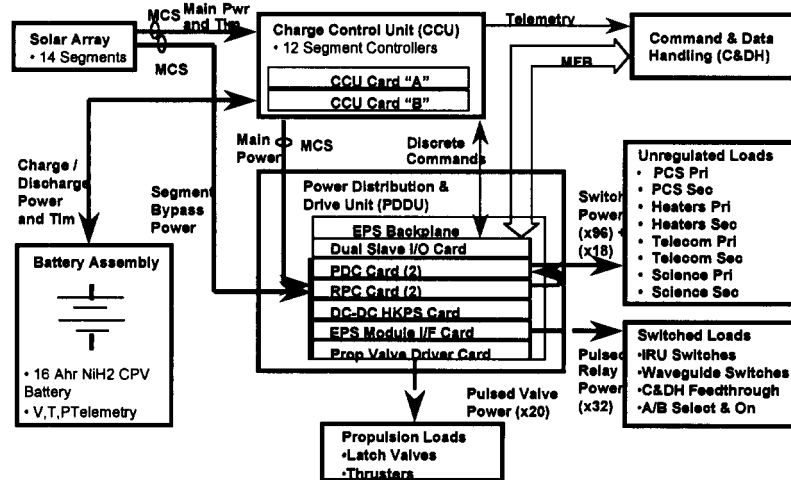


Figure 5. Power Generation and Distribution Subsystem Block Diagram

**In-Flight Performance.** The PG&D performance from launch through the first several months of the nominal mission has been within expectations. The pre-launch battery temperature was elevated and very close to the 24 °C red limit. Fortunately, the battery was charged at a lower temperature during countdown allowing comfortable margin. The battery performed superbly during liftoff, ascent, and initial acquisition. At Launch+55 minutes, the solar panels were illuminated as expected, and the batteries were recharged within the next hour. The batteries have been on trickle charge ever since, with a 106% state of charge.

Observatory power loads have been within 5% of pre-launch predictions. The maximum load observed in flight (with full heater power and the IRAC instrument powered on) has been 425 W, the minimum load (in safe mode) has been 253 W, and the average load has been 375 W. Comparing the average load to the maximum array power yields an average solar array utilization of about 75%.

## TELECOMMUNICATIONS SUBSYSTEM (Telecom)

**Subsystem Overview.** The Spitzer X-band Telecom subsystem provides the link by which the Observatory exchanges data with the Deep Space Network (DSN) ground stations during command uplinks and data downlinks. The system utilizes X-band channel 13, transmitting at 8413.641975 MHz and receiving at 7161.156636 MHz. In addition to communications, the system provides two-way coherent Doppler tracking for orbit determination. The Telecom subsystem is designed for an operational lifetime of 5.2 years to provide communications capability to a maximum Observatory distance of 0.64 astronomical units (AU). The Telecom subsystem consists of the following components:

**Low Gain Antenna (LGA).** Spitzer has four LGAs (two receiving patch antennas and two transmitting patch antennas). The LGAs were designed for use during off-nominal conditions, initial acquisition, In-Orbit Checkout (IOC), and Safe Mode events. They provide nearly 360° spherical coverage at all mission ranges for emergency communications with the Observatory at 7.8125 bps uplink and 40 bps downlink.

**High Gain Antenna (HGA).** Nominal communications take place through the HGA. The HGA link is capable of supporting an uplink rate of 2000 bps at a range of 0.64 AU on 70m DSN stations and 0.32 AU on 34m stations. The HGA supports the maximum downlink rate of 2.2 Mbps out to 0.32 AU on 70m DSN stations.

**Small Deep Space Transponder (SDST).** The SDST is the Observatory terminal to the DSN, which provides the interface between the DSN ground stations, the Telecom subsystem, and the spacecraft C&DH subsystem. For redundancy, Spitzer has two SDSTs.

**Solid-State Power Amplifier (SSPA).** Spitzer has two SSPAs to amplify the modulated SDST output signal (~12 dBm) to 15 W in a single-SSPA configuration or 29 W in a dual-SSPA configuration.

**Miscellaneous Hardware.** Spitzer also contains waveguide transfer switches, diplexers, filters, and couplers. The cross strapping of these components allows for various configurations and increases the overall subsystem reliability.

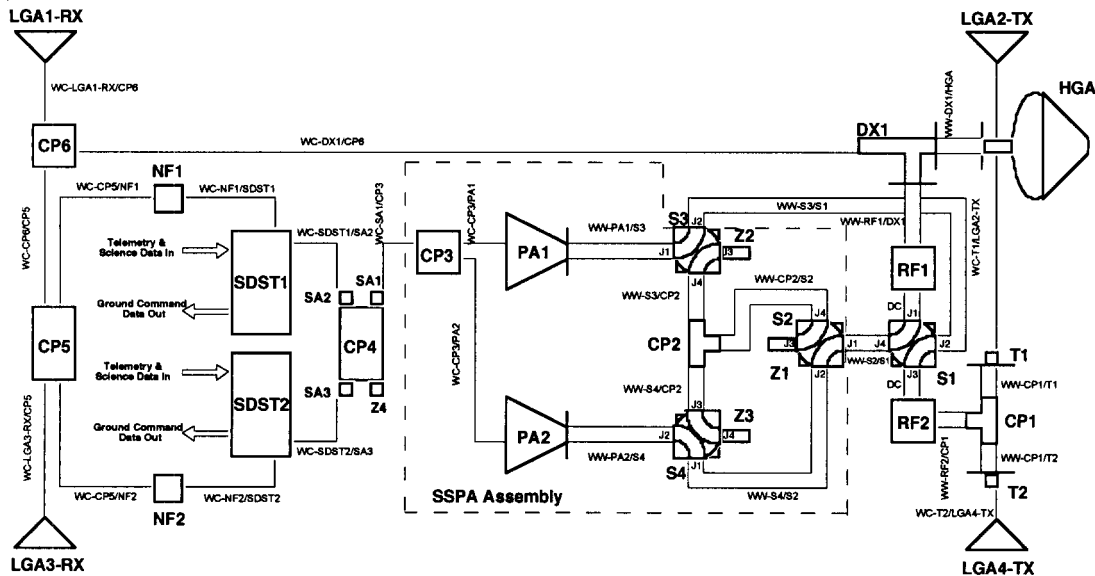


Figure 6. Telecommunication Subsystem Schematic

**In-Flight Performance.** The Spitzer Telecom subsystem has performed to expectations. The pre-launch predictions for link margins and data rates closely resemble performance to date and the system has maintained nominal status throughout various anomalous events. Several different uplink and downlink rates have been demonstrated successfully in flight. The transition to the HGA occurred about 21 days after launch. This transition initially revealed an unexpectedly low signal level of approximately -124 dBm. However, a power check performed later revealed that this was merely a measurement artifact, and that the actual signal level was above predictions by 0.6 dB. By verifying the downlink signal level, the predicted telecom performance was validated and shown to meet the project requirements.

## THERMAL CONTROL SUBSYSTEM (TCS)

**Subsystem Overview.** TCS provides spacecraft temperature control and monitoring. In addition to keeping all spacecraft components within their individual temperature ranges, TCS must maintain a very low heat input interface to the CTA. TCS is also required to maintain the spacecraft bus structure at a very uniform temperature in order to reduce misalignment between the star trackers and the telescope. Thermal control is maintained by using computer controlled heaters, heat pipes, high and low emittance surface finishes, multi-layer insulation, high and low conductivity materials, and temperature sensors. Block or functional redundancy is required for all active components and the system operates autonomously without ground commands during normal operations. Temperature sensors provide temperature telemetry at regular intervals for spacecraft health and safety monitoring.

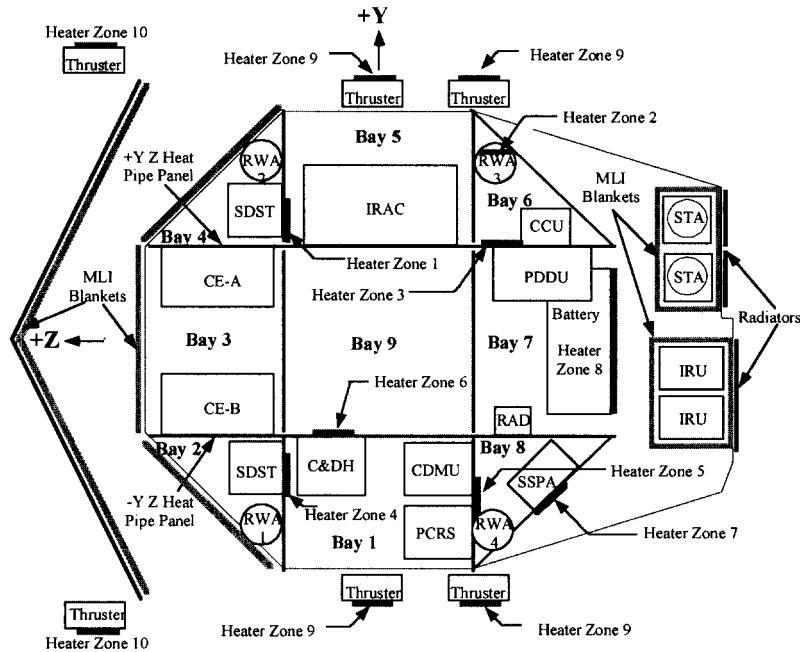


Figure 7. Thermal Control Subsystem Components and Implementation

**Development Challenges.** It had been recognized in the early planning stages of the program that a major program challenge would be to minimize the heat leak into the liquid helium cryostat thus providing for a long duration mission. The S/C bus and solar panel thermal interfaces with the CTA were critical. The solar panel is radiatively decoupled from the CTA by several layers of multi-layer insulation and an aluminum solar panel radiation shield. All of this contributes to a low effective emissivity and minimal radiation heat leak into the CTA. A similar shielding technique is used for the top deck of the bus to shield it from the bottom of the telescope. Low thermal conductivity struts are used to mount the telescope to the spacecraft bus and minimize conduction heat leak.

The second thermal challenge was to maintain an isothermal structure to minimize thermal distortion, particularly important for star tracker accuracy. Structural deflections due to thermal gradients would cause a misalignment between the telescope and the star trackers, which would result in pointing inaccuracies. To maintain an isothermal structure, heat pipes were imbedded in the structural panels to distribute heat from warm areas to cold areas. Similarly, the upper deck contains a heat pipe that attaches to each of the CTA strut mounting pads in order to maintain a pad temperature difference of no greater than 1 °C.

**In-Flight Performance.** The TCS has performed very well on orbit. All spacecraft components are within their desired temperature ranges and are operating near their predicted temperatures. The TCS design has also proven to be very flexible. In one case, reaction wheel heater settings were raised from -26 °C to 5 °C to provide improved pointing control performance.

## SPACECRAFT FLIGHT SOFTWARE (FSW)

**Subsystem Overview.** The FSW stores, validates, prioritizes, and distributes commands throughout the Observatory and provides for the coordination and execution of tasks. It provides autonomous operations capability, as well as the ability to control all Observatory functions from the ground. The FSW resides in the spacecraft C&DH, and controls or interfaces with all of the Observatory subsystems. The FSW is written in C language, and consists of approximately 125,000 lines of code.

A critical feature of the FSW is to ensure spacecraft survival without ground intervention during anomalous situations. Fault Protection (FP) maintains Observatory health and safety, protecting Spitzer's ability to accomplish its mission objectives in the presence of hardware and software failures, extreme environments such as solar flares, and ground system errors. The FP is built upon three principles: a) fault avoidance, b) fault detection/isolation/recovery, and c) fault tolerance. Fault avoidance is achieved through the design, manufacturing, and assembly practices that prevent the

fault from occurring. Fault detection/isolation/recovery is the autonomous or ground-directed short-term reactions that prevent faults from occurring. Fault tolerance results from the design practices that mitigate the long-term impacts of faults. All Spitzer subsystems are single fault tolerant.

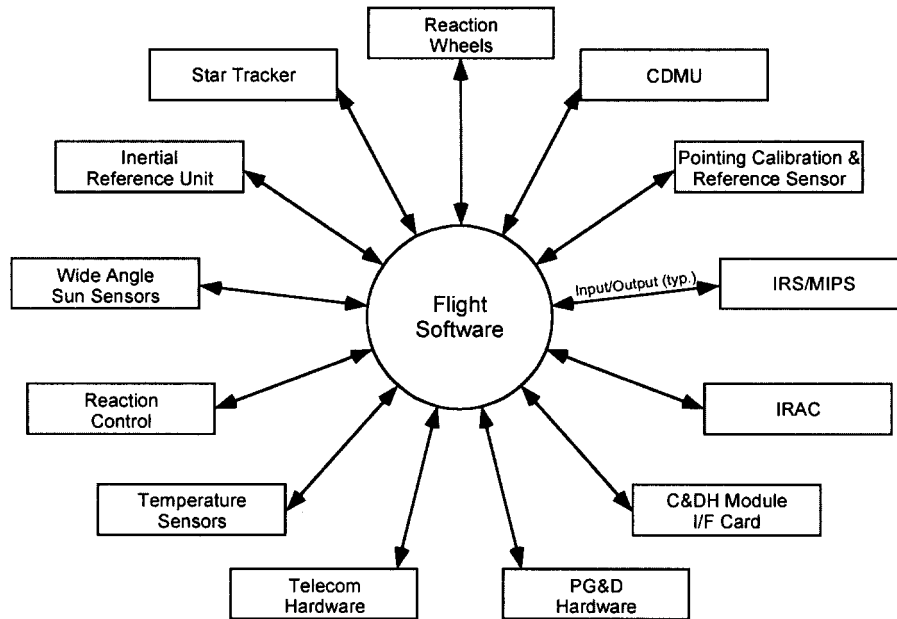


Figure 8. Flight Software Top Level Context Diagram

**Development Challenges.** Spitzer FSW experienced difficult challenges in its development. One significant problem was the extensive planned usage of heritage code. Due to budgetary reasons, the development goal was to maximize the amount of reused FSW. This was possible in some cases, but in most areas adapting heritage code to Spitzer requirements proved complex. Frequently, new code had to be written and thoroughly tested where heritage code had been previously envisioned. Two other challenges resulted from the extremely precise pointing requirements and the unprecedented throughput of data for Spitzer. Each of these resulted in a two-part dilemma: FSW code had to be developed or modified to meet Spitzer-specific design requirements, and new ground models had to be created to accurately simulate spacecraft system level responses. Developing both in parallel was difficult because of the heavy interdependence.

**In-Flight Performance.** Spitzer FSW has performed nominally and met all mission requirements. Processor utilization, a concern during development, has averaged only 52%. Data storage on the Mass Memory Card (MMC), also a concern during development, has been effectively managed by the ground process and has not resulted in any problems. The FP design has proven to be reliable, responding properly when required.

## CRYOGENIC TELESCOPE ASSEMBLY (CTA)

**Subsystem Overview.** Spitzer was designed to be launched with the telescope at ambient temperature, a scheme different from that of previous cryogenic telescopes. Spitzer's warm launch architecture takes advantage of the Earth-trailing solar orbit, which eliminates the heat load from the Earth, and also requires a smaller and lighter cryostat. Throughout the expected mission lifetime of more than 5 years, the CTA will provide a 5.5K primary mirror and a 1.2K cold sink to the science instruments. The CTA consists of the outer shell group, the 0.85-meter Ritchey-Chrétien telescope assembly, the superfluid helium cryostat, and the multiple instrument chamber.

**Outer Shell Group.** The outer shell group includes the outer shell, outer vapor-cooled shield, thermal shields to block radiation from the spacecraft and solar panel, miniature electrical cables, and the CTA-to-spacecraft interface structure. Effectively a large radiative cooler running at 34K, the outer shell surrounds the telescope and cryostat and rejects heat to space. The outer vapor-cooled shield sits between the outer shell and telescope reducing radiation from the outer shell to the telescope. The CTA solar panel shield and spacecraft shield block the outer shell from view of the warm spacecraft bus and solar panel. The outer shell is mounted to, but thermally isolated

from, the spacecraft by means of low-conductivity struts and miniature ribbon cables. Struts and cables are vapor cooled by attachment to the helium vent line independent of the outer vapor-cooled shield.

**Telescope Assembly.** The telescope assembly, including the primary and secondary mirrors, metering tower, bulkhead, focus mechanism, and barrel baffle is thermally and structurally mounted to the outside of the cryostat vacuum shell. The telescope is cooled by helium effluent from the cryostat. The telescope must be 5.5K, the temperature necessary for the MIPS long wavelength detector to achieve its desired performance.

**Cryostat.** The cryostat comprises the vacuum shell, tank support struts, two vapor-cooled shields, aperture door mechanism, photon shutter mechanism, superfluid helium tank, and plumbing associated with helium management. The fluid management system consists of internal and external valve manifolds. In flight, the vacuum shell is at 5.5K, so parasitic heat loads to the helium tank are almost negligible. The helium tank includes a makeup heater, which is used to control telescope temperature. Since there is so little parasitic heating on the cryogen bath, the makeup heater is used to increase the helium vent rate to cool the telescope with the vapor.

**Multiple Instrument Chamber (MIC).** The MIC houses the three science instruments and the PCRS, and is mounted on top of the helium tank.

**Cryogenic Mechanisms.** The CTA has four cryogenic mechanisms. The photon shutters are used to block radiation coming through the cryostat aperture and to provide a low background inside the MIC for ground testing. The dust cover attached to the outer shell at launch was successfully ejected four days after launch. The aperture door provides a vacuum seal to the cryostat vacuum shell during ground testing. The focus mechanism, mounted behind the telescope secondary mirror, provides a focus range of  $\pm 25$  mm at the telescope focal surface.

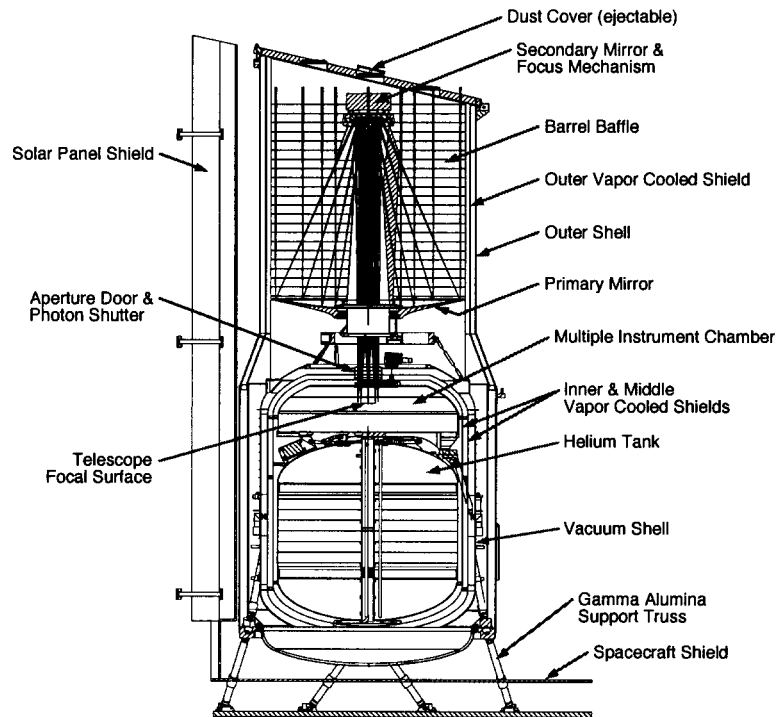


Figure 9. Cryogenic Telescope Assembly Components

**In-Flight Performance.** The performance of the CTA mechanisms has been completely nominal. The photon shutters were successfully opened during the launch countdown and are not operated in flight. The dust cover was successfully ejected four days after launch, and the aperture door was opened five days after launch. The focus mechanism was adjusted in flight during telescope cool-down to find the optimum focus position, where it will remain for the rest of the mission. No future operations of the CTA mechanisms are planned for the remainder of the mission.

The CTA thermal performance has also been nominal. The telescope cooled down to its operating temperature of 5.5K at 41 days after launch and without consuming a significant amount of helium. The telescope cooling profile matched well with the pre-launch analytical predictions, so that the schedule of IOC activities was not interrupted. The superfluid helium tank is providing the science instrument cold assemblies with a cold sink temperature of 1.24K, which meets the 1.2 – 1.4K requirement. The makeup heater on the cryostat tank has proven to be useful in controlling

helium flow rate, and has been used successfully to vary the telescope temperature with instrument operations to conserve helium.

The Spitzer mission life is tied to the cryogen lifetime. In-flight mass gauge measurements have resulted in a helium lifetime prediction of 4.0 – 5.8 years, with the range due to the uncertainty in the measurement. Future mass gauge measurements will reduce the uncertainty. In comparison to the lifetime requirement of 2.7 years and the design goal of 5.2 years, the helium usage rate promises a lengthy and successful Spitzer mission.

## FUTURE PLANS

There are no more critical events in the Spitzer mission plan, and therefore no significant mission risks in the future. However, because the helium consumption limits the lifetime of the Observatory, the engineering team is constantly looking for ways to improve the overall science efficiency. Several items are in discussion including the following: increase the interval between STA-to-PCRS calibrations from 8 to 12 hours, reduce the duration of the STA-to-PCRS calibrations, increase the interval between the IRU calibrations from 72 to 96 hours, reduce the duration of the IRU calibrations, improve the sequencing architecture, and increase the PCS maximum torque to improve slew performance. If any of these future enhancements are pursued, they will be tested thoroughly prior to implementation on the Observatory.

## CONCLUSION

In summary, the engineering systems of the Spitzer Space Telescope are performing superbly. All performance requirements are being met, and the science community is extremely happy with the quality and the quantity of the infrared science data collected so far. There are no significant issues that threaten the health and safety of the Observatory. By all means of measure, Spitzer has been a tremendous success and promises to continue its achievements well beyond the 2.7-year mission requirement.

## ACKNOWLEDGEMENTS

The authors would like to thank all the members of the development team and the flight team for their support. This includes team members from the Jet Propulsion Laboratory, Lockheed Martin Space Systems Company, Ball Aerospace & Technology Corp., and the members of the science community. In particular, the authors would like to acknowledge the following individuals for their direct contributions to this paper: Bill Adams, John Delk, Brian Dempsey, Mark Effertz, Paul Finley, Bill Jackson, Angus McMechen, John Miles, Rob Mock, Larry Padgett, Dan Swanson, John Tietz, Nick Vadlamudi, and Carl Yanari.

## ACRONYM LIST

AU	Astronomical Unit	LGA	Low Gain Antenna
C&DH	Command & Data Handling	MIC	Multiple Instrument Chamber
CCU	Charge Control Unit	MIPS	Multiband Imaging Photometer for Spitzer
CDMU	CTA Driver Multiplexer Unit	MMC	Mass Memory Card
CMIC	C&DH Module Interface Card	NASA	National Aeronautics & Space Administration
CTA	Cryogenic Telescope Assembly	PCRS	Pointing Calibration and Reference Sensor
DSN	Deep Space Network	PCS	Pointing Control Subsystem
FP	Fault Protection	PDDU	Power Distribution & Drive Unit
FPC	Flight Processor Card	PG&D	Power Generation and Distribution Subsystem
FSW	Flight Software	Pin	P-type—intrinsic—N-type
FULDL	Fast Uplink Downlink	PPIC	Payload & PCS Interface Card
GCF	Gyroscope Calibration Filter	RCS	Reaction Control Subsystem
HGA	High Gain Antenna	RWA	Reaction Wheel Assembly
IOC	In-Orbit Checkout	S/C	Spacecraft
IRAC	Infrared Array Camera	SDST	Small Deep Space Transponder
IRS	Infrared Spectrograph	SIRTF	Space Infrared Telescope Facility
IRU	Inertial Reference Unit	SSPA	Solid State Power Amplifier

STA Star Tracker Assembly  
SV Science Verification

TCS Thermal Control Subsystem  
WASS Wide Angle Sun Sensor

## REFERENCES

- [1] J. Miles and N. Vadlamudi, *Observatory Description Document – Space Infrared Telescope Facility*, LMMS/P458569, 674-SEIT-300, Version 1.2, November 1, 2002.